



## Aminosilylene-bridged *ansa*-zirconocenes for branched polyethylenes with bimodal molecular weight distributions

Yonggyu Han<sup>a</sup>, Hyoseok Kim<sup>a</sup>, Min Hyung Lee<sup>b</sup>, Youngjo Kim<sup>c</sup>, Junseong Lee<sup>a</sup>, Yoon Sup Lee<sup>a</sup>, Youngkyu Do<sup>a,\*</sup>

<sup>a</sup> Department of Chemistry, KAIST, Daejeon 305-701, Republic of Korea

<sup>b</sup> Department of Chemistry, University of Ulsan, 680-749, Republic of Korea

<sup>c</sup> Department of Chemistry and Basic Science Research Institute, Chungbuk National University, Cheongju, Chungbuk 361-763, Republic of Korea

### ARTICLE INFO

#### Article history:

Received 26 June 2009

Received in revised form 1 September 2009

Accepted 3 September 2009

Available online 6 September 2009

#### Keywords:

Bimodal molecular weight distribution

Branched polyethylene

*Ansa*-metallocene

Aminosilylene-bridge

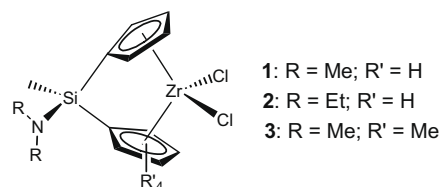
### ABSTRACT

Reactions of the dilithium salt of aminosilylene-bridged ligands with  $(\text{Me}_2\text{N})_2\text{ZrCl}_2(\text{THF})_2$  followed by the treatment of  $\text{Me}_3\text{SiCl}$  are found to be an efficient synthetic route to aminosilylene-bridged *ansa*-zirconocenes,  $\text{R}_2\text{N}(\text{Me})\text{Si}(\eta^5\text{-C}_5\text{H}_4)_2\text{ZrCl}_2$  ( $\text{R} = \text{Me}$  (**1**),  $\text{Et}$  (**2**)) and  $\text{Me}_2\text{N}(\text{Me})\text{Si}(\eta^5\text{-C}_5\text{H}_4)(\eta^5\text{-C}_5\text{Me}_4)\text{ZrCl}_2$  (**3**). Crystal structure of **3** determined by X-ray diffraction study reveals the presence of  $\pi$ -bonding interaction between N and Si atoms, which is further supported by DFT calculation results. These complexes are very active ( $>1 \times 10^3 \text{ Kg}/(\text{mol Cat} \cdot \text{atm} \cdot \text{h})$ ) for homopolymerization of ethylene in the presence of methylalumoxane (MAO) cocatalyst, generating polyethylenes that contain branches as well as bimodal molecular weight distribution (MWD). Methyl, ethyl, butyl, and other longer branches ( $n \geq 6$ ) are observed in the resulting polyethylenes. The polyethylenes from **1**, **2** and **3**/MAO show a broad MWD range (6.3–42.2, 3.5–4.0 and 2.6–3.4, respectively).

© 2009 Elsevier B.V. All rights reserved.

### 1. Introduction

Metallocene-based polyethylene (PE) possesses excellent properties such as high clarity and high impact strength [1,2], but its bulk production has been hampered by significant processing problems due to a lack of branching and narrow molecular weight distribution (MWD). Thus, the enhancement of the processibility of metallocene-based PE has become an important research subject in recent years, with particular focus on introducing branches and modulating the MWD. The former objective has been approached via copolymerization with higher  $\alpha$ -olefins [3], the use of mono- [4] and bi-nuclear [5] “constrained geometry catalysts”, the use of *meso* *ansa*-metallocene-based catalysts [6], and homopolymerization with “tandem catalytic systems” [7]. The latter goal has been tackled by using mixed metallocene systems [8], and by designing metallocene precatalysts that produce multi catalytically active species during the polymerization process [9–11]. In order to develop metallocene catalytic system that can simultaneously carry out both functions of the formation of branches and the modulation of the MWD, we have designed functionalized silylene-bridged *ansa*-zirconocenes **1–3**.



The purpose of introducing  $\text{NR}_2$  group to the bridging Si atom is three-fold. Firstly, the amine group is expected to cause the alteration of the electron donating ability of the *ansa*-ligands in point via direct  $\pi$ -bonding interaction between the lone pair electrons of N atom and the Si orbital. The foregoing electronic effect may lead to a change in polymerization process. Secondly, in the ethylene polymerization with methylalumoxane (MAO), the amine group is also expected to interact with the cocatalyst without causing steric encumbrance to a metal center, generating dual active species and thereby resulting in bimodal MWD of PE. Thirdly, even though group 4 metallocenes bearing amine groups have attracted interest from strategic viewpoint in developing new catalytic systems, the amine groups were only introduced to the cyclopentadienyl ring fragments as demonstrated in the following examples of *rac*- $\text{Me}_2\text{Si}(2\text{-}(N,N\text{-dimethylamino})\text{indenyl})_2\text{ZrCl}_2$  (I) [12],  $(9\text{-}(N,N\text{-dimethylamino})\text{fluorenyl})_2\text{ZrCl}_2$  (II) [13] and  $\text{Me}_2\text{Si}(\text{cyclopentadienyl})(3\text{-}(N,N\text{-dimethylaminoethyl})\text{cyclopentadienyl})\text{ZrCl}_2$  (III) [11]

\* Corresponding author.

E-mail address: ykdo@kaist.ac.kr (Y. Do).

and (1-(*p*-*N,N*-dimethylaminophenyl)-3,4-dimethylcyclopentadienyl)<sub>2</sub>ZrCl<sub>2</sub> (IV) [14]. While the modulation of MWD of PE by III/MAO and the isospecific stereocontrol in propylene polymerization by IV/MAO were unambiguously achieved by means of the direct interaction of the amine group with MAO, the electronic and/or steric effect of the amine groups that locate near the metal center have often led to a long induction period for I or lower activity for II and III due to the amine interaction with the metal center. In this paper, we report the synthesis, characterization, and polymerization behavior of functionalized silylene-bridged *ansa*-zirconocenes **1–3** that constitute the first examples of highly active, metallocene precatalysts being capable of generating branched polyethylenes with broad MWD.

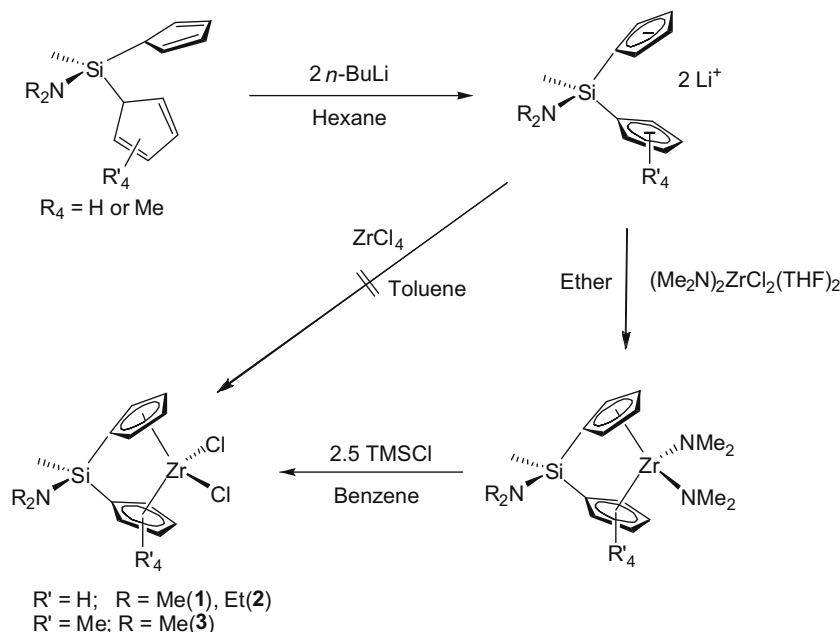
## 2. Results and discussion

### 2.1. Synthesis and molecular structure of aminosilylene-bridged *ansa*-zirconocenes, **1–3**

Synthetic route to the compounds **1–3** is depicted in Scheme 1. The sequential treatment of MeSiCl<sub>3</sub> with lithium cyclopentadienylide and 2 equiv. of R<sub>2</sub>NH (R = Me, Et) afforded the corresponding aminosilylene-bridged ligands in quantitative yields. Direct metal-

lations with ZrCl<sub>4</sub> were unsuccessful while the combined use of (Me<sub>2</sub>N)<sub>2</sub>ZrCl<sub>2</sub>(THF)<sub>2</sub> and TMSCl was very efficient [15]. The obtained crystalline compounds **1–3** are very soluble in toluene, CH<sub>2</sub>Cl<sub>2</sub>, and ethereal solvents.

The crystal structure of **3** has been determined and two views of the molecular structure along with the selected interatomic distances and angles are illustrated in Fig. 1. The perspective top view and the structural parameters clearly reveal the presence of  $\pi$ -bonding interaction between N and Si atoms. The coplanarity of the dimethylaminosilylene constituents Si, N, C(16), and C(17) atoms as indicated by the sum of 358.4° for three angles around the N atom and the short N–Si distance of 1.705(3) Å compared to the usual N–Si single bond distance of 1.80 Å [16] are strong indication of the foregoing  $\pi$ -bonding interaction between N and Si atoms. According to the DFT calculation results, the N–Si bonding orbital is highly polarized toward N atom and the lone pair electrons of the N atom strongly interact with  $\sigma^*$  orbital of the Si–C(15) bond, confirming the presence of  $\pi$ -bonding interaction as observed in the crystal structure (Fig. 2) [17]. Actually, this interaction leads to a slight lengthening of Si–C(15) distance (1.869(4) Å) in **3** in comparison with that of the reported Si–C bond (1.852(4) Å) [18]. Other structural features of **3** such as the dihedral angle of 58.72° between two cyclopentadienyl rings, the



Scheme 1. Synthetic route of aminosilylene-bridged *ansa*-zirconocenes.

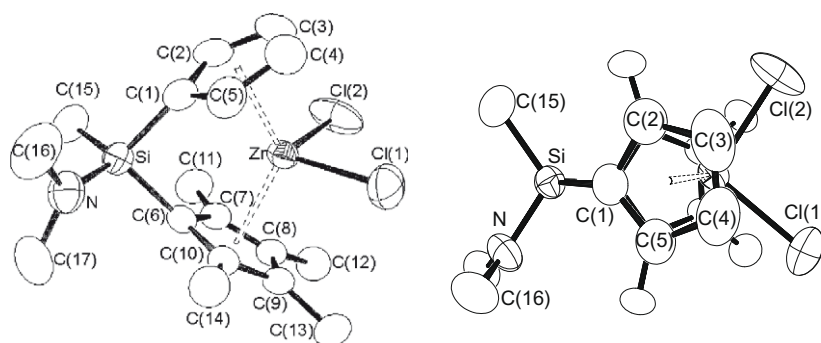


Fig. 1. Molecular structure of **3** (top; side view, bottom; top view, 50% thermal ellipsoids). H-atoms were omitted for clarity. Selected bond distances (Å) and angles (°): Zr–C(1) 2.487(3), Zr–C(2) 2.497(3), Zr–C(3) 2.556(3), Zr–C(4) 2.561(3), Zr–C(5) 2.483(3), Si–N 1.705(3), Si–C(15) 1.869(4), C(16)–N–Si 123.7(3), C(17)–N–Si 121.8(2), C(16)–N–C(17) 113.4(3),  $\angle(Cp-Cp')$  58.72.

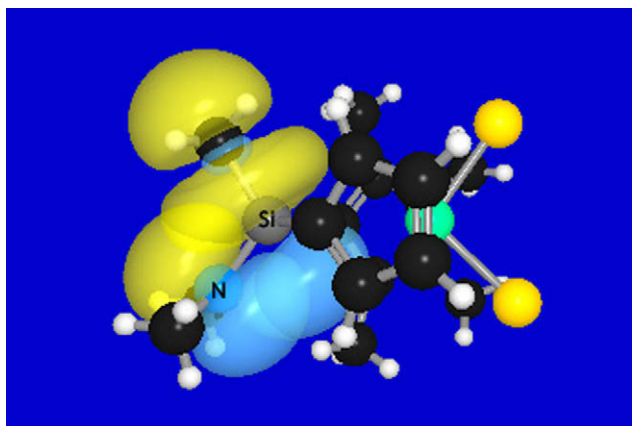


Fig. 2. Pre-NBOs representing  $\pi$ - $\sigma^*$  interaction in the N-Si bond of **3** (NBO: natural bond orbital).

C(1)-Si-C(6) angle of  $95.7^\circ$ , the Cn(1)-Zr-Cn(2) angle of  $127.5^\circ$ , and the Cn-Zr distances are not unusual and similar to those for  $\text{Me}_2\text{Si}(\eta^5\text{-C}_5\text{H}_4)(\eta^5\text{-C}_5\text{Me}_4)\text{ZrCl}_2$  (**5**) [19], a prototypical complex of **3**, thus indicating that the introduction of an amino group on the Si bridge does not significantly affect the steric environment around the zirconium center.

## 2.2. Ethylene polymerization

The aminosilylene-bridged *ansa*-zirconocenes **1–3** were used as precatalysts in ethylene polymerizations in the presence of MAO at various polymerization temperatures ( $T_p$ ). The polymerization results for **1–3**/MAO systems are summarized in Table 1. Comparative ethylene polymerization using non-aminosilylene complexes **4** and **5** as precatalyst was also carried out under the same polymerization condition at  $70^\circ\text{C}$ . For all **1–3**/MAO systems tested in ethylene polymerizations, the catalytic activity reaches a maximum at  $70^\circ\text{C}$  with values greater than  $1 \times 10^3$  Kg/(mol Cat. $\cdot$ atm $\cdot$ h) without an induction period. Even though these complexes show lower activity than **4** and **5**/MAO ( $2.5 \times 10^3$  Kg/(mol Cat. $\cdot$ atm $\cdot$ h) and  $2.2 \times 10^3$  Kg/(mol Cat. $\cdot$ atm $\cdot$ h), respectively), the activity is within the same order of magnitude. In **1–3**/MAO systems, both the activity and the  $M_w$  of bis-Cp systems **1** and **2**/MAO are lower than those of **3**/MAO which have a  $\text{Me}_4\text{Cp}$  ring fragment instead of

a Cp. Since the comparative result of the non-aminosilylene bridged **4** and **5** reported previously shows quite similar activity and  $M_w$  between two systems [20], this result appears to imply the presence of an additional effect that may involve with the aminosilylene-bridge in **1–3**/MAO. All the catalysts show decreasing  $M_w$  as  $T_p$  increases, except for the  $M_w$  for **1**/MAO at  $50^\circ\text{C}$  which is higher than that obtained at  $30^\circ\text{C}$ . Among bis-Cp systems, the aminosilylene-bridged **1** and **2**/MAO show both the lower activity and  $M_w$  than **4**/MAO system at  $70^\circ\text{C}$ , indicating an much electron deficient nature of active species while the difference between **1** and **2**/MAO is not marked except for the greater MWD from **1**/MAO than that from **2**/MAO (runs 3, 7, and 13). Interestingly, the broad MWD and decreased  $T_m$  from **1** and **2**/MAO systems with the conspicuous dependence of  $T_m$  on  $T_p$  are quite different from those observed for **4**/MAO although the  $T_m$  observed at high  $T_p$ , i.e.  $70$  and  $90^\circ\text{C}$  could also be slightly affected by the low  $M_w$  [21]. For example, the DSC thermograms of the PEs produced by **2**/MAO exhibit the apparent decrease of  $T_m$  from the value typical of HDPE ( $T_m > \sim 125^\circ\text{C}$ ) to the value of LLDPE ( $T_m < \sim 125^\circ\text{C}$ ) as  $T_p$  increases (runs 5–8). However, in the case of **3**/MAO systems, the MWD and  $T_m$  observed at all temperatures are within relatively narrow ranges and the overall results including activity are very similar between each other (runs 11 and 14).

## 2.3. $^{13}\text{C}$ NMR analysis of polyethylenes

The  $^{13}\text{C}$  NMR spectra of the PEs produced by **1** and **2**/MAO at various  $T_p$  reveal the remarkable introduction of methyl, ethyl, butyl, and other longer branches ( $n \geq 6$ ), depending on  $T_p$  (Table 2, Fig. 3 and Fig. S2 in Supplementary material). For the **2**/MAO system, the signals due to ethyl branches, i.e. the  $1\text{B}_2$ ,  $2\text{B}_2$ , and  $\text{brB}_2$  carbon signals at 11.2, 26.6, and 39.6 ppm, respectively, are clearly visible at  $30^\circ\text{C}$  but diminish as  $T_p$  increases (Fig. 3b–e). On the other hand, the signals due to methyl branches ( $1\text{B}_1$  and  $\text{brB}_1$  carbon signals at 19.9 and 33.2 ppm, respectively), butyl branches ( $4\text{B}_4$ ,  $\alpha\text{B}_4$ , and  $\text{brB}_4$  carbon signals at 34.0, 34.5, and 38.2 ppm, respectively), and other longer branches increase in intensity as  $T_p$  increases [22]. The branching seems to reach a maximum at  $90^\circ\text{C}$ ; the PE obtained at this  $T_p$  has 0.17% of methyl branches, 0.16% of butyl branches, and 2.15% of other branches [23]. The  $T_p$  dependence of branching for the **1**/MAO system is slightly different from that of the **2**/MAO, in that the ethyl branches are present for all  $T_p$ , and in that methyl branching as well as overall branching

Table 1  
Ethylene polymerization results<sup>a</sup>.

Run no.	Cat.	$T_p$ ( $^\circ\text{C}$ )	Polymer (g)	$A^d$	$M_w^e$ ( $\times 10^3$ )	$M_w/M_n^e$	$T_m^f$ ( $^\circ\text{C}$ )
1	<b>1</b>	30	0.15	118	67.8	20.4	129.0
2		50	1.02	850	114.3	42.2	129.4
3		70	1.54	1232	10.1	6.3	123.1
4	<b>2</b>	90	0.97	776	9.9	6.6	124.0
5		30	0.39	186	98.9	3.6	131.1
6		50	1.06	795	21.0	4.0	128.2
7		70	1.74	1134	7.2	3.5	121.8
8		90	0.94	750	5.5	3.5	118.8
9	<b>3</b>	30	0.9	744	173	2.9	132.7
10		50	1.2	976	57.9	2.6	133.6
11		70	1.7	1344	35.1	2.7	131.5
12	<b>4</b> <sup>b</sup>	90	1.1	848	14.1	3.4	127.6
13		70	2.2	2460	83.8	2.7	130.8
14	<b>5</b> <sup>c</sup>	70	2.8	2240	17.0	2.2	131.2

<sup>a</sup> Polymerization conditions: P(ethylene) = 1 bar, [Cat.] = 5  $\mu\text{mol}$ , [Al/Zr] = 2000,  $t_p$  = 15 min, solvent = 50 mL of toluene.

<sup>b</sup> **4** =  $\text{Me}_2\text{Si}(\eta^5\text{-C}_5\text{H}_4)_2\text{ZrCl}_2$ ; polymerization conditions: P(ethylene) = 1 bar, [Cat.] = 5  $\mu\text{mol}$ , [MAO/Cat.] = 2000,  $t_p$  = 15 min, solvent = 50 mL of toluene.

<sup>c</sup> **5** =  $\text{Me}_2\text{Si}(\eta^5\text{-C}_5\text{H}_4)(\eta^5\text{-C}_5\text{Me}_4)\text{ZrCl}_2$ .

<sup>d</sup> Activity in units of Kg/(mol Cat. $\cdot$ bar h).

<sup>e</sup> Determined by GPC.

<sup>f</sup> Determined by DSC.

**Table 2**  
Branches in polymers<sup>a</sup>.

Run no.	Cat.	$T_p$ (°C)	Methyl branch (%)	Ethyl branch (%)	Butyl branch (%)	Other branch (%)	Total branching (%)
1	1	50	0.07	0	0.13	0.26	0.46
2		70	0.15	0	0.26	4.28	4.69
3		90	0.10	0	0.25	4.13	4.48
4	2	30	0.07	0.02	0.07	0.72	0.88
5		50	0.08	0	0.08	1.48	1.64
6		70	0.19	0	0.10	1.96	2.25
7	3	90	0.17	0	0.16	2.15	2.48
8		90	0.09	0	0.06	2.09	2.24

<sup>a</sup> Calculated the percentage of branching based on <sup>13</sup>C NMR's of the resulting polyethylenes.

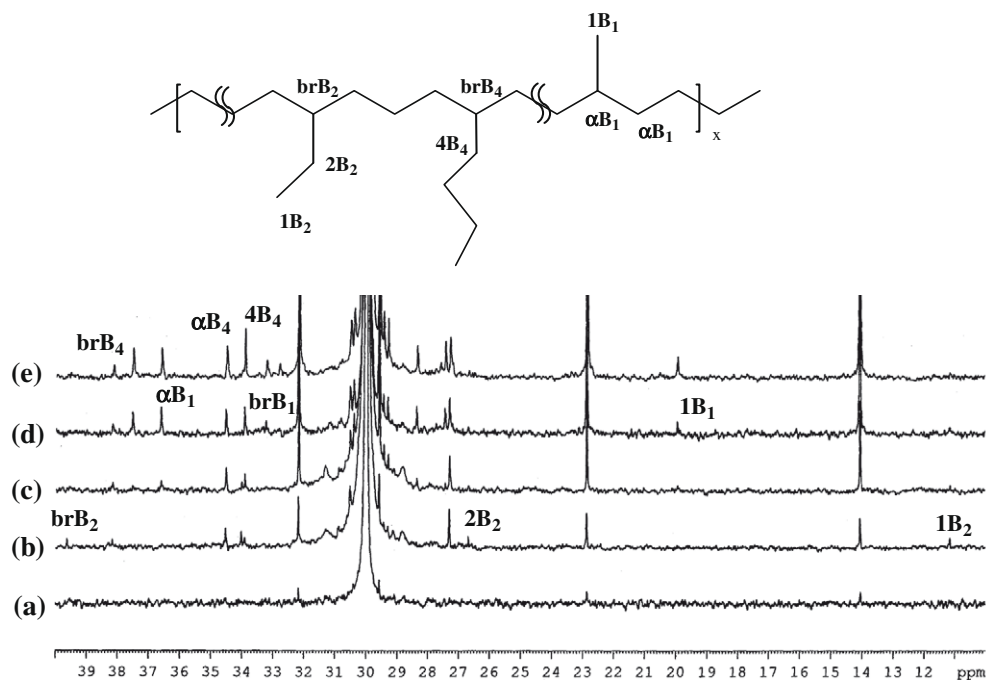


**Fig. 3.** <sup>13</sup>C NMR spectra of polyethylenes obtained at  $T_p$  = (a) 70 °C from **4**/MAO, (b) 30 °C, (c) 50 °C, (d) 70 °C, (e) 90 °C from **2**/MAO.

reach their maxima at 70 °C (Fig. S2 in Supplementary material). It is interesting to note that the  $T_p$  at which maximum branching occurs coincides with the  $T_p$  at which the minimum  $T_m$  results in for both catalytic systems. Furthermore, the <sup>13</sup>C NMR spectrum of the PE obtained at 90 °C from **3**/MAO systems reveals the similar presence of some short chain branches although the  $T_m$  belongs to the range of HDPE (Fig. S4 in Supplementary material). In contrast, the <sup>13</sup>C NMR spectrum of the PE from **4**/MAO shows just ends group carbon signals typical for linear PE (Fig. 3a).

These observations of the branched polymers with **1–3**/MAO systems are most likely due to the electronic effect of the  $R_2N(Me)$ -Si-bridge rather than steric influence, which is further supported by the comparative results from the non-aminosilylene complexes **4** and **5** and the similar structural features of **3** with **5**. According to the theoretical calculations for ethylene polymerization [24], it is reported that the enhanced electrophilicity of an active center is favorable to generate vinyl-terminated macromonomers. Thus, the formation of the branched polymers from **1–3**/MAO systems can be explained by the consequence of facile formation of vinyl-terminated macromonomers due to the increased electrophilicity of the metal centers. Regarding methyl branch, for example, it can be suggested that initial  $\beta$ -hydride abstraction from the  $\beta$ -carbon of a polymer chain is followed by rotation of the unsaturated chain end (chain-isomerization), and then 2,1-reinsertion into

the Zr–H bond. In metallocene-catalyzed olefin polymerization, the chain-isomerization is observed in the form of not only the *trans*-vinylene group in ethylene polymerization [25] but [*mrrm*] stereoregions in propylene polymerization [26]. Actually, methyl [25,27] and ethyl branches [5,6] via chain-isomerization are detected in the specific metallocene systems from a single ethylene monomer feed. However, butyl and longer branches result from the incorporation of the macromonomer generated during polymerization into a growing polymer chain [28].

The overall polymerization results of the aminosilylene-bridged **1**, **2**, and **3**/MAO systems described above are in good agreement with the involvement of highly electrophilic zirconium center in polymerization. Therefore, it can be strongly suggested that the interaction of the amino group of  $R_2N(Me)$ -Si-bridge with the Al components of cocatalyst results in the reduction of electron density at the metal center although the interacting Lewis acidic species are not clearly defined. Recently, our group reported that Lewis acidic Al components can interact with the amino group attached on the substituent of Cp ligand in the form of either free alkylaluminum or MAO anion [14]. Furthermore, these interactions seem to be quite dependent on the steric environment at the bridge. The less extent of branching formation and the relatively narrow MWD as well as the higher activity and  $M_w$  from the more sterically hindered,  $Me_4Cp$ -substituted **3**/MAO system could be the

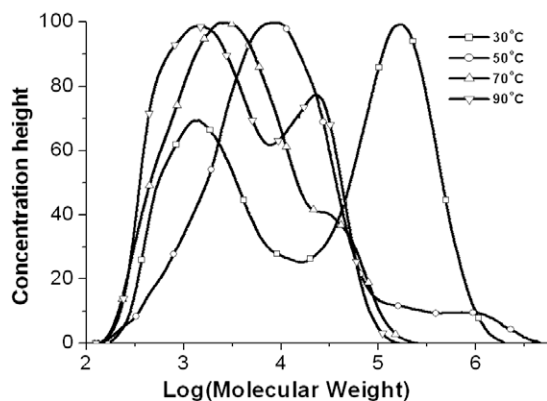


Fig. 4. MWDs of polyethylenes produced by **1**/MAO.

consequence of the weak Al–N interactions that can exert only marginally an electron withdrawing effect on the metal center. A similar explanation might be valid for the  $\text{NEt}_2$ -substituted **2**/MAO system which showed the less broad MWD than the  $\text{NMe}_2$ -substituted **1**/MAO although the overall polymerization results including branching are very similar between two systems in ethylene polymerization.

#### 2.4. Influence of aminosilylene-bridge on bimodal MWD

The catalytic system **1**/MAO produces PE with a broad MWD range (6.3–42.2) while **2** and **3**/MAO produce PE with relatively narrow MWD ranges (3.5–4.0, and 2.6–3.4, respectively). Inspection of the MWDs of the resulting polymers reveals bimodal distributions for **1**/MAO at all  $T_p$  with asymmetric tails (Fig. 4) and the appearance of shoulder at high  $T_p$  for **2**, and **3**/MAO. From the fact that **4** and **5**/MAO produce PE having a narrow and unimodal MWD, respectively, this unusual aspect of MWD from the aminosilylene-bridged *ansa*-zirconocenes can be ascribed to the catalytically multi-active species generated *in situ* during ethylene polymerization by the Lewis acid–base interactions between the Al components of cocatalyst and the nitrogen atom of the bridge unit [11,14]. The  $^1\text{H}$  and  $^{13}\text{C}$  NMR spectroscopic monitoring of solutions containing complex **1** and Lewis acids provides an indirect evidence that confirms the presence of such an interaction (Fig. 5 and Fig. S5 in Supplementary material). When  $\text{AlMe}_3$  was employed as a Lewis acid in toluene- $d_8$  at ambient temperature, the change in the spectrum was immediate; the resulting spectrum is rather complicated but indicates an interaction between the amino group of complex **1** and  $\text{AlMe}_3$  as well as instant alkylation (Fig. S6 in Supplementary material). The use of the bulky Lewis

acid  $\text{B}(\text{C}_6\text{F}_5)_3$  in benzene- $d_6$  leads more obviously to the slow appearance of an additional set of signals, illustrated in Fig. 5, assignable to the Lewis acid–base adduct  $\mathbf{1}\cdot\text{B}(\text{C}_6\text{F}_5)_3$ .

### 3. Conclusions

We have demonstrated that the introduction of  $\text{NR}_2$  group into the bridging Si atom of silylene-bridged *ansa*-zirconocenes can lead to highly active catalytic systems being capable of producing branched polyethylene with broad MWD upon MAO activation. *In situ* formation of multi-component catalytic active species through the possible Lewis acid–base interaction between the amino group and the Al components of cocatalyst might be responsible for the unusual polymerization results, holding promise as a new class of metallocene catalysts for the development of easy processing metallocene polyolefins.

### 4. Experimental

#### 4.1. General considerations

All operations were performed under an inert dinitrogen atmosphere using Glove-box and standard Schlenk techniques. THF, toluene, *n*-hexane, and *n*-pentane were distilled from Na–K alloy,  $\text{Et}_2\text{O}$  from Na-benzophenone ketyl, and  $\text{CH}_2\text{Cl}_2$  from  $\text{CaH}_2$ . Dimethylamine, diethylamine,  $\text{MeSiCl}_3$ ,  $\text{Me}_3\text{SiCl}$  (TMSCl), and *n*-butyllithium (2.5 M solution in *n*-hexanes) were purchased from Aldrich and  $\text{LiC}_5\text{H}_5$ ,  $\text{LiC}_5\text{Me}_4\text{H}$ , and tetrakis(dimethylamino)zirconium ( $\text{Zr}(\text{NMe}_2)_4$ ) from Strem.  $\text{Me}_2\text{Si}(\eta^5\text{-C}_5\text{H}_4)_2\text{ZrCl}_2$  (**4**) [29],  $\text{Me}_2\text{Si}(\eta^5\text{-C}_5\text{H}_4)(\eta^5\text{-C}_5\text{Me}_4)\text{ZrCl}_2$  (**5**) [29],  $(\text{Me}_2\text{N})_2\text{ZrCl}_2(\text{THF})_2$  [30],  $\text{MeSi}(\text{C}_5\text{H}_5)_2\text{Cl}$  [31], and  $\text{MeSi}(\text{C}_5\text{Me}_4\text{H})(\text{C}_5\text{H}_5)\text{Cl}$  [31] were prepared according to the literature procedures. MAO was supplied by Chemtura. Deuterated solvents ( $\geq 99$  atom%D) were purchased from Cambridge Isotope Laboratories, dried over activated molecular sieves (4 Å) and used after vacuum transfer to Schlenk tubes equipped with J. Young valves.  $^1\text{H}$  and  $^{13}\text{C}$  NMR spectra were recorded on a Bruker AM 300 or a Bruker Spectrospin 400 spectrometer at room temperature and were referenced to the residual peaks of the  $\text{CDCl}_3$  (7.24 ppm for  $^1\text{H}$  NMR and 77.0 ppm for  $^{13}\text{C}\{^1\text{H}\}$  NMR) and benzene- $d_6$  (7.15 ppm for  $^1\text{H}$  NMR and 120.12 ppm for  $^{13}\text{C}\{^1\text{H}\}$  NMR). Elemental analyses were performed on an EA 1110-FISONS (CE Instruments) at KAIST.

#### 4.2. $\text{Me}_2\text{N}(\text{Me})\text{Si}(\eta^5\text{-C}_5\text{H}_4)_2\text{ZrCl}_2$ (**1**)

The reaction of  $\text{ClMeSi}(\text{C}_5\text{H}_5)_2$  and 2 equiv. of  $\text{Me}_2\text{NH}$  in THF at 0 °C, followed by removal of ammonium salt over the Celite-pad and vacuum drying of the filtrate, quantitatively gave oily  $\text{Me}_2\text{N}$

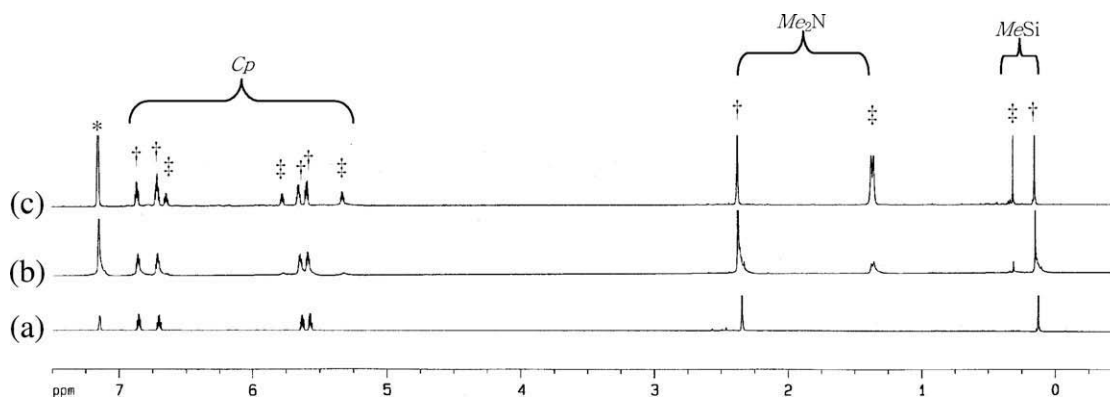


Fig. 5.  $^1\text{H}$  NMR spectroscopic monitoring of complex **1** and  $\text{B}(\text{C}_6\text{F}_5)_3$  in  $\text{C}_6\text{D}_6$ . (a)  $t < 5$  min, (b)  $t > 3$  h, (c)  $t > 24$  h. \*:  $\text{C}_6\text{D}_6$ , †: complex **1**, ‡: adduct  $\mathbf{1}\cdot\text{B}(\text{C}_6\text{F}_5)_3$ .

(Me)Si(C<sub>5</sub>H<sub>5</sub>)<sub>2</sub>. The lithiation of Me<sub>2</sub>N(Me)Si(C<sub>5</sub>H<sub>5</sub>)<sub>2</sub> with 2 equiv. of *n*-BuLi in hexane at –78 °C afforded the dilithium salt as a white powder that was kept in a Glove-box for further use. To a precooled (–78 °C) solid mixture of dilithium salt of the ligand (8.0 mmol, 1.8 g) and an equimolar amount of (Me<sub>2</sub>N)<sub>2</sub>ZrCl<sub>2</sub>(THF)<sub>2</sub> (3.2 g) was added slowly 40 mL of Et<sub>2</sub>O with vigorous stirring for 1 h. Then, the reaction mixture was slowly allowed to warm to room temperature and stirred overnight, giving an orange solution with white precipitate. Filtration through Celite-pad followed by removal of the solvent *in vacuo* gave sticky orange oil. The sticky oil was dissolved with 30 mL of benzene and treated with 2.5 equiv. of TMSCl at 0 °C. The reaction mixture was allowed to warm to room temperature and then stirred for 30 min. After evaporation of the solvent, the extract of the solid residue with *n*-hexane (30 mL) was stored at –20 °C overnight, giving 0.67 g of **1** as white microcrystals (22%). Me<sub>2</sub>N(Me)Si(η<sup>5</sup>-C<sub>5</sub>H<sub>4</sub>)<sub>2</sub>Zr(NMe<sub>2</sub>)<sub>2</sub>: <sup>1</sup>H NMR (400.13 MHz, C<sub>6</sub>D<sub>6</sub>, ppm): δ = 6.60 (m, 1H, C<sub>5</sub>H<sub>4</sub>), 6.53 (m, 1H, C<sub>5</sub>H<sub>4</sub>), 5.87 (m, 1H, C<sub>5</sub>H<sub>4</sub>), 5.69 (m, 1H, C<sub>5</sub>H<sub>4</sub>), 2.81 (s, 6H, (CH<sub>3</sub>)<sub>2</sub>NZr), 2.75 (s, 6H, (CH<sub>3</sub>)<sub>2</sub>NZr), 2.63 (s, 6H, (CH<sub>3</sub>)<sub>2</sub>NSi), 0.39 (s, 3H, CH<sub>3</sub>Si). <sup>13</sup>C{<sup>1</sup>H} NMR (100.62 MHz, C<sub>6</sub>D<sub>6</sub>, ppm): δ = 118.93, 115.95, 113.19, 111.76, 110.51, 49.12, 48.64, 37.69, –5.99. Me<sub>2</sub>N-(Me)Si(η<sup>5</sup>-C<sub>5</sub>H<sub>4</sub>)<sub>2</sub>ZrCl<sub>2</sub>: <sup>1</sup>H NMR (400.13 MHz, CDCl<sub>3</sub>, ppm): δ = 7.00 (m, 1H, C<sub>5</sub>H<sub>4</sub>), 6.87 (m, 1H, C<sub>5</sub>H<sub>4</sub>), 6.03 (m, 1H, C<sub>5</sub>H<sub>4</sub>), 5.92 (m, 1H, C<sub>5</sub>H<sub>4</sub>), 2.77 (s, 6H, (CH<sub>3</sub>)<sub>2</sub>NSi), 0.59 (s, 3H, CH<sub>3</sub>Si). <sup>13</sup>C{<sup>1</sup>H} NMR (100.62 MHz, CDCl<sub>3</sub>, ppm): δ = 130.86, 125.99, 116.66, 113.76, 110.92, 37.36, –5.67. *Anal. Calc.* for C<sub>13</sub>H<sub>17</sub>NSiCl<sub>2</sub>Zr: C, 41.36; H, 4.54; N, 3.71. Found: C, 41.69; H, 4.77; N, 3.60%.

#### 4.3. Et<sub>2</sub>N(Me)Si(η<sup>5</sup>-C<sub>5</sub>H<sub>4</sub>)<sub>2</sub>ZrCl<sub>2</sub> (**2**)

The white compound **2** was prepared by the reaction of dilithium salt of Et<sub>2</sub>N(Me)Si(C<sub>5</sub>H<sub>5</sub>)<sub>2</sub> (8.0 mmol, 2.1 g) and an equimolar amount of (Me<sub>2</sub>N)<sub>2</sub>ZrCl<sub>2</sub>(THF)<sub>2</sub> (3.2 g) in a manner analogous to the procedure for the compound **1** (2.0 g, 60%). Et<sub>2</sub>N(Me)Si(η<sup>5</sup>-C<sub>5</sub>H<sub>4</sub>)<sub>2</sub>Zr(NMe<sub>2</sub>)<sub>2</sub>: <sup>1</sup>H NMR (400.13 MHz, C<sub>6</sub>D<sub>6</sub>, ppm): δ = 6.60 (m, 1H, C<sub>5</sub>H<sub>4</sub>), 6.51 (m, 1H, C<sub>5</sub>H<sub>4</sub>), 5.90 (m, 1H, C<sub>5</sub>H<sub>4</sub>), 5.71 (m, 1H, C<sub>5</sub>H<sub>4</sub>), 3.06 (m, 4H, (CH<sub>3</sub>CH<sub>2</sub>)<sub>2</sub>NSi), 2.83 (s, 6H, (CH<sub>3</sub>)<sub>2</sub>NZr), 2.75 (s, 6H, (CH<sub>3</sub>)<sub>2</sub>NZr), 1.03 (t, 6H, (CH<sub>3</sub>CH<sub>2</sub>)<sub>2</sub>NSi), 0.45 (s, 3H, CH<sub>3</sub>Si). <sup>13</sup>C{<sup>1</sup>H} NMR (100.62 MHz, C<sub>6</sub>D<sub>6</sub>, ppm): δ = 119.15, 115.60, 113.65, 112.07, 110.36, 49.16, 48.62, 39.71, 15.63, –3.53. Et<sub>2</sub>N-(Me)Si(η<sup>5</sup>-C<sub>5</sub>H<sub>4</sub>)<sub>2</sub>ZrCl<sub>2</sub>: <sup>1</sup>H NMR (400.13 MHz, CDCl<sub>3</sub>, ppm): δ = 7.02 (m, 1H, C<sub>5</sub>H<sub>4</sub>), 6.85 (m, 1H, C<sub>5</sub>H<sub>4</sub>), 6.04 (m, 1H, C<sub>5</sub>H<sub>4</sub>), 5.93 (m, 1H, C<sub>5</sub>H<sub>4</sub>), 3.17 (q, 4H, (CH<sub>3</sub>CH<sub>2</sub>)<sub>2</sub>NSi), 1.16 (t, 6H, (CH<sub>3</sub>CH<sub>2</sub>)<sub>2</sub>NSi), 0.62 (s, 3H, CH<sub>3</sub>Si). <sup>13</sup>C{<sup>1</sup>H} NMR (100.62 MHz, CDCl<sub>3</sub>, ppm): δ = 131.24, 125.43, 117.16, 113.34, 111.39, 39.27, 15.38, –3.70. *Anal. Calc.* for C<sub>15</sub>H<sub>21</sub>NSiCl<sub>2</sub>Zr: C, 44.4; H, 5.21; N, 3.45. Found: C, 43.4; H, 5.41; N, 3.45%.

#### 4.4. Me<sub>2</sub>N(Me)Si(η<sup>5</sup>-C<sub>5</sub>H<sub>4</sub>)(η<sup>5</sup>-C<sub>5</sub>Me<sub>4</sub>)ZrCl<sub>2</sub> (**3**)

The yellow compound **3** was prepared by the reaction of the dilithium salt of Et<sub>2</sub>N(Me)Si(C<sub>5</sub>H<sub>5</sub>)(C<sub>5</sub>Me<sub>4</sub>H) (8.0 mmol, 2.1 g) and an equimolar amount of (Me<sub>2</sub>N)<sub>2</sub>ZrCl<sub>2</sub>(THF)<sub>2</sub> (3.2 g) in a manner analogous to the procedure for the compound **1** (1.9 g, 54%). <sup>1</sup>H NMR (400.13 MHz, CDCl<sub>3</sub>, ppm): δ = 7.05 (m, 1H, C<sub>5</sub>H<sub>4</sub>), 6.92 (m, 1H, C<sub>5</sub>H<sub>4</sub>), 5.69 (m, 1H, C<sub>5</sub>H<sub>4</sub>), 5.66 (m, 1H, C<sub>5</sub>H<sub>4</sub>), 2.71 (s, 6H, (CH<sub>3</sub>)<sub>2</sub>NSi), 2.02 (s, 3H, C<sub>5</sub>(CH<sub>3</sub>)<sub>4</sub>), 2.00 (s, 3H, C<sub>5</sub>(CH<sub>3</sub>)<sub>4</sub>), 1.97 (s, 3H, C<sub>5</sub>(CH<sub>3</sub>)<sub>4</sub>), 1.85 (s, 3H, C<sub>5</sub>(CH<sub>3</sub>)<sub>4</sub>), 0.69 (s, 3H, CH<sub>3</sub>Si). <sup>13</sup>C{<sup>1</sup>H} NMR (100.62 MHz, CDCl<sub>3</sub>, ppm): δ = 137.82, 134.53, 129.31, 127.71, 125.46, 124.28, 111.99, 108.35, 113.76, 100.45, 36.86, 15.02, 13.15, 12.04, 11.76, –1.79. *Anal. Calc.* for C<sub>17</sub>H<sub>33</sub>NSiCl<sub>2</sub>Zr: C, 47.09; H, 5.80; N, 3.23. Found: C, 46.74; H, 5.66; N, 3.13%.

**Table 3**  
Crystallographic data for **3**.

Compound	<b>3</b>
Empirical formula	C <sub>17</sub> H <sub>25</sub> Cl <sub>2</sub> NSiZr
Formula weight	433.59
Crystal system	Monoclinic
Space group	P2 <sub>1</sub> /c
<i>a</i> (Å)	9.5798(9)
<i>b</i> (Å)	16.5651(16)
<i>c</i> (Å)	12.0865(12)
β (°)	92.225(2)
<i>V</i> (Å <sup>3</sup> )	1916.6(3)
<i>Z</i>	4
<i>D</i> <sub>calc</sub> (g/cm <sup>3</sup> )	1.503
<i>F</i> (0 0 0)	888
<i>T</i> (K)	293(2)
μ (Mo Kα) (mm <sup>-1</sup> )	0.71073
θ Range (°)	2.09–27.99
Number of unique reflections	4264
Number of observed reflections ( <i>I</i> > 2σ( <i>I</i> ))	3228
Number of parameters refined	206
<i>R</i> <sub>1</sub> ( <i>I</i> > 2σ( <i>I</i> )) <sup>a</sup>	0.0385
<i>wR</i> <sub>2</sub> (all data) <sup>b</sup>	0.1053
Goodness-of-fit (GOF)	1.024
ρ <sub>fin</sub> (max./min.) (e Å <sup>-3</sup> )	–0.744, +0.524

<sup>a</sup> *R*<sub>1</sub> = ||*F*<sub>o</sub>|| – ||*F*<sub>c</sub>|| / ||*F*<sub>o</sub>||.

<sup>b</sup> *wR*<sub>2</sub> = [(*w*(*F*<sub>o</sub><sup>2</sup> – *F*<sub>c</sub><sup>2</sup>))<sup>2</sup> / (*w*(*F*<sub>o</sub><sup>2</sup>))<sup>2</sup>]<sup>1/2</sup>.

#### 4.5. X-ray structure determination of **3**

Crystallographic data were collected on a Bruker SMART 1K-CCD area detector diffractometer with a graphite-monochromated Mo Kα radiation (λ = 0.71073 Å) at 293 K. The hemisphere of diffraction data were collected as ω scan frames with a width of 0.3°/frame and exposure time of 10 s/frame. Cell parameters were determined and refined by SMART program [32]. Data reduction and Lorentz polarization correction were performed using SAINT software [33], but any correction for crystal decay was not required. Empirical absorption correction was applied with SADABS program [34]. The structure was solved by direct method and refined by full matrix least-squares methods using the SHELXTL program package with anisotropic thermal parameters for all non-hydrogen atoms. Hydrogen atoms were placed at their geometrically calculated positions and refined riding on the corresponding carbon atoms with isotropic thermal parameters. The detailed crystallographic data for **3** are listed in Table 3.

#### 4.6. Ethylene polymerization

Into a well-degassed 250 mL-Schlenk flask with magnetic stirring, freshly distilled toluene (39 mL) and MAO (in toluene solution, 6.0 mL, Al/Zr = 2000) was transferred via cannula. The temperature was adjusted to a constant (30, 50, 70, and 90 °C) using an external bath and the ethylene monomer was saturated at 1 bar after degassing with it several times. The polymerization was started by the injection of a toluene solution of catalyst (5.0 mL, 5 μmol). All the polymerizations were quenched by the addition of MeOH (10 mL) after the given reaction time. The resulting polyethylene was precipitated by adding 10% HCl solution of MeOH (100 mL) followed by 100 mL of MeOH. After stirring for 1 h, the solid polyethylene was filtered and washed with MeOH several times, and then dried under vacuum overnight at 70 °C.

#### 4.7. Polymer analysis

<sup>13</sup>C NMR spectra of the polymers were recorded on a Bruker Avance 400 spectrometer in 1,3,5-trichlorobenzene: benzene-*d*<sub>6</sub> (v/v = 8/2) with reference to the residual peak of benzene-*d*<sub>6</sub>

( $\delta = 120.12$ ) at 100 °C [22]. Molecular weight and molecular weight distribution of polymers were determined by GPC (Waters 150C, 135 °C) in 1,2,4-trichlorobenzene using polystyrene columns as standards. Melting temperatures ( $T_m$ ) of the polymers were measured by differential scanning calorimeter (DSC, TA Instrument) under nitrogen atmosphere at a heating rate of 10 °C/min. The *n*-heptane-soluble fraction of polyethylene from Soxhlet extraction was considered as a low-molecular-weight polyethylene.

#### 4.8. Computational details

Natural bond orbital (NBO) analysis [35] was performed to investigate the N–Si bond character in **3** for the X-ray structure with the DFT method using the B3LYP functional [36] and the 6-31G\* basis set [37] for all atoms other than the Zr atom for which the Stuttgart RSC 1997 ECP [38] was used. NBO analysis was carried out using GAUSSIAN 03 program [39] and NBO 5.G package [40]. The NBOVIEW program [41] created 3D graphical images of electronic orbitals produced by the NBO program. The detailed analysis results are summarized in the Supplementary material.

#### Acknowledgements

Financial support from the Korea Science and Engineering Foundation is gratefully acknowledged. The authors thank Honam Petrochemical Corp. for GPC analysis and Dr. Jeong-Wook Hwang for his assistance in characterizing the molecular structure of **3**.

#### Appendix A. Supplementary material

CCDC 219743 (**3**) contains the supplementary crystallographic data for this paper. These data can be obtained free of charge from The Cambridge Crystallographic Data Centre via [www.ccdc.cam.ac.uk/data\\_request/cif](http://www.ccdc.cam.ac.uk/data_request/cif). Supplementary data associated with this article can be found, in the online version, at doi:10.1016/j.jorganchem.2009.09.003.

#### References

- [1] For a review of ethylene polymerization, see: H.G. Alt, A. Köppl, Chem. Rev. 100 (2000) 1205.
- [2] A.K. Kulshrestha, S. Tarapatra, in: C. Vasile (Ed.), Handbook of Polyolefins, Marcel Dekker, New York, 2000, pp. 1–70.
- [3] (a) C. Przybyla, B. Tesche, G. Fink, Macromol. Rapid Commun. 20 (1999) 328; (b) A. Yano, S. Hasegawa, T. Kaneko, M. Sone, M. Sato, A. Akira, Macromol. Chem. Phys. 200 (1999) 1542.
- [4] (a) K. Kunz, G. Erker, S. Döring, R. Fröhlich, G. Kehr, J. Am. Chem. Soc. 123 (2001) 6181; (b) Y.-X. Chen, T.J. Marks, Organometallics 16 (1997) 3649; (c) K. Soga, T. Uozumi, S. Nakamura, T. Toneri, T. Teranishi, T. Sano, T. Arai, Macromol. Chem. Phys. 197 (1996) 4237; (d) D.D. Devorce, F.J. Timmers, D.L. Hasha, R.K. Rosen, T.J. Marks, P.A. Deck, C.L. Stern, Organometallics 14 (1995) 3132; (e) J.C. Stevens, Proc. MetCon Huston, 1993, pp. 157–170.; (f) J.M. Canich, Eur. Patent Appl. EP 420 436-A1, 1991 (Exxon Chemical Co.); (g) J.C. Stevens, F.J. Timmers, D.R. Wilson, G.F. Schmidt, P.N. Nickias, R.K. Rosen, G.W. Knight, S. Lai, Eur. Patent Appl. EP 416 815-A2, 1991 (Dow Chemical Co.).
- [5] L. Li, M.V. Metz, H. Li, M.C. Chen, T.J. Marks, L. Liable-Sands, A.L. Rheingold, J. Am. Chem. Soc. 124 (2002) 12725.
- [6] (a) G. Melillo, L. Izzo, M. Zinna, C. Tedesco, L. Oliva, Macromolecules 35 (2002) 9256; (b) Y. Yuan, L. Wang, L. Feng, Polym. Int. 49 (2000) 1289.
- [7] (a) Z.J.A. Komon, G.C. Bazan, Macromol. Rapid Commun. 22 (2001) 467; (b) Z.J.A. Komon, X. Bu, G.C. Bazan, J. Am. Chem. Soc. 122 (2000) 1830.
- [8] (a) A.H. Dekmezian, E.J. Markel, W. Weng, P. Jiang, Proc. MetCon Huston, 2001, Session V.; (b) L. Dagnillo, J.B.P. Soares, A. Penlidis, J. Polym. Sci., Part A: Polym. Chem. 36 (1998) 831; (c) A.E. Hamielec, J.B.P. Soares, Prog. Polym. Sci. 21 (1996) 651.
- [9] Y. Kim, Y. Han, M.H. Lee, S.W. Yoon, K.H. Choi, B.G. Song, Y. Do, Macromol. Rapid Commun. 22 (2001) 573.
- [10] H.G. Alt, R. Ernst, J. Mol. Catal. A-Chem. 195 (2003) 11.
- [11] C. Muller, D. Lilje, M.O. Kristen, P. Jutzi, Angew. Chem. Int. Ed. 39 (2000) 789.
- [12] E. Barsties, S. Schaible, M.-H. Prosenc, U. Rief, W. Röhl, O. Wayand, B. Dorer, H.-H. Brintzinger, J. Organomet. Chem. 520 (1996) 63.
- [13] S.A. Miller, J.E. Bercaw, Organometallics 19 (2000) 5608.
- [14] (a) S.K. Kim, H.K. Kim, M.H. Lee, S.W. Yoon, Y. Do, Chem. Eur. J. 13 (2007) 9107; (b) S.K. Kim, H.K. Kim, M.H. Lee, S.W. Yoon, Y. Do, Angew. Chem. Int. Ed. 45 (2006) 6163.
- [15] J.N. Christopher, G.M. Diamond, R.F. Jordan, J.L. Petersen, Organometallics 15 (1996) 4038.
- [16] R. Tacke, U. Wannagat, Bioactive Organo-Silicon Compounds, Springer-Verlag, New York, 1979.
- [17] See the Supporting Information for details.
- [18] P.J. Chirik, L.M. Henling, J.E. Bercaw, Organometallics 20 (2001) 534.
- [19] (a) A. Antiñolo, I. López-Solera, A. Otero, S. Prashar, A.M. Rodríguez, E. Villaseñor, Organometallics 20 (2001) 71; (b) G. Tian, B. Wang, X. Dai, S. Xu, X. Zhou, J. Sun, J. Organomet. Chem. 634 (2001) 145.
- [20] A. Antiñolo, I. López-Solera, A. Otero, S. Prashar, A.M. Rodríguez, E. Villaseñor, Organometallics 21 (2002) 2460.
- [21] (a) W.M. Leung, R.St. John Manley, A.R. Panaras, Macromolecules 18 (1985) 753; (b) G.M. Stack, L. Mandelkern, I.G. Voigt-Martin, Macromolecules 17 (1984) 321.
- [22] (a) G.B. Galland, R. Quijada, R. Rojas, G.C. Bazan, Z.J.A. Komon, Macromolecules 35 (2002) 339; (b) J.C. Randall, Rev. Macromol. Chem. Phys. C29 (1989) 201.
- [23] The proportions of branches were calculated by using the method described in Ref. [21b]; The <sup>13</sup>C NMR spectrum of the *n*-heptane insoluble fraction (more than 85%) of the PE in question was employed in these calculations.
- [24] (a) P. Margl, L. Deng, T. Ziegler, J. Am. Chem. Soc. 121 (1999) 154; (b) P. Margl, L. Deng, T. Ziegler, Organometallics 17 (1998) 933.
- [25] P. Lehmus, E. Kokko, R. Leino, H.J.G. Luttikhedde, B. Rieger, J.V. Seppälä, Macromolecules 33 (2000) 8534.
- [26] (a) M.K. Leclerc, H.H. Brintzinger, J. Am. Chem. Soc. 118 (1996) 9024; (b) M.K. Leclerc, H.H. Brintzinger, J. Am. Chem. Soc. 117 (1995) 1651.
- [27] W.-J. Wang, D. Yan, S. Zhu, E. Hamielec, Macromolecules 31 (1998) 8677.
- [28] (a) E. Kolodka, W.-J. Wang, P.A. Charpentier, S. Zhu, A.E. Hamielec, Polymer 41 (2000) 3985; (b) A. Malmberg, J. Liimatta, A. Lehtinen, B. Löfgren, Macromolecules 32 (1999) 6687.
- [29] C.S. Bajgur, W.R. Tikkanen, J.L. Petersen, Inorg. Chem. 24 (1985) 2539.
- [30] E. Benzing, W. Kornicker, Chem. Ber. 94 (1961) 2263.
- [31] P.J. Shapiro, W.D. Cotter, W.P. Schaefer, J.A. Labinger, J.E. Bercaw, J. Am. Chem. Soc. 116 (1994) 4623.
- [32] SMART, Version 5.0, Data Collection Software, Bruker AXS, Inc., Madison, WI, 1998.
- [33] SAINT, Version 5.0, Data Integration Software, Bruker AXS, Inc., Madison, WI, 1998.
- [34] G.M. Sheldrick, SADABS, Program for Absorption Correction with the Bruker SMART System, Universität Göttingen, Germany, 1996.
- [35] A.E. Reed, L.A. Curtiss, F. Weinhold, Chem. Rev. 88 (1988) 899.
- [36] (a) A.D. Becke, J. Chem. Phys. 98 (1993) 5648; (b) C.T. Lee, W.T. Yang, R.G. Parr, Phys. Rev. B 37 (1998) 785.
- [37] (a) W.J. Hehre, R. Ditchfield, J.A. Pople, J. Chem. Phys. 56 (1972) 2257; (b) P.C. Hariharan, J.A. Pople, Theor. Chim. Acta 28 (1973) 213.
- [38] D. Andrae, U. Haeussermann, M. Dolg, H. Stoll, H. Preuss, Theor. Chim. Acta 77 (1990) 123.
- [39] GAUSSIAN 03, Revision C.02, M.J. Frisch, G.W. Trucks, H.B. Schlegel, G.E. Scuseria, M.A. Robb, J.R. Cheeseman, J.A. Montgomery Jr., T. Vreven, K.N. Kudin, J.C. Burant, J.M. Millam, S.S. Iyengar, J. Tomasi, V. Barone, B. Mennucci, M. Cossi, G. Scalmani, N. Rega, G.A. Petersson, H. Nakatsuji, M. Hada, M. Ehara, K. Toyota, R. Fukuda, J. Hasegawa, M. Ishida, T. Nakajima, Y. Honda, O. Kitao, H. Nakai, M. Klene, X. Li, J.E. Knox, H.P. Hratchian, J.B. Cross, V. Bakken, C. Adamo, J. Jaramillo, R. Gomperts, R.E. Stratmann, O. Yazyev, A.J. Austin, R. Cammi, C. Pomelli, J.W. Ochterski, P.Y. Ayala, K. Morokuma, G.A. Voth, P. Salvador, J.J. Dannenberg, V.G. Zakrzewski, S. Dapprich, A.D. Daniels, M.C. Strain, O. Farkas, D.K. Malick, A.D. Rabuck, K. Raghavachari, J.B. Foresman, J.V. Ortiz, Q. Cui, A.G. Baboul, S. Clifford, J. Cioslowski, B.B. Stefanov, G. Liu, A. Liashenko, P. Piskorz, I. Komaromi, R.L. Martin, D.J. Fox, T. Keith, M.A. Al-Laham, C.Y. Peng, A. Nanayakkara, M. Challacombe, P.M.W. Gill, B. Johnson, W. Chen, M.W. Wong, C. Gonzalez, J.A. Pople, Gaussian, Inc., Wallingford CT, 2004.
- [40] NBO 5.G., E.D. Glendening, J.K. Badenhoop, A.E. Reed, J.E. Carpenter, J.A. Bohmann, C.M. Morales, F. Weinhold, Theoretical Chemistry Institute, University of Wisconsin, Madison, 2001.
- [41] NBOVIEW 1.0, M. Wendt, F. Weinhold, Theoretical Chemistry Institute, University of Wisconsin, Madison, 2001.